SECOND EUROPEAN CONFERENCE ON EARTHQUAKE ENGINEERING
AND SEISMOLOGY, ISTANBUL AUG. 25-29, 2014

SLOPE STABILITY ANALYSIS UNDER SEISMIC LOADING

Sahar Ismail[1], Fadi Hage Chehade[2] and Riad Al Wardany[1]

ABSTRACT

Soil slope analysis has attracted the attention of researchers and engineers over the years. The analysis of soil slopes is essential to evaluate their performance and stability under seismic loading. The overstress of a slope or the reduction in the shear strength of the sloped soil may cause the soil matrix to displace and thus jeopardizes public safety. In general, two indicators of performance are considered by the engineers in the analysis of the stability of soil slopes under seismic loading: the lateral deformation of the soil slope and the safety factor against failure. Lebanon and the Mediterranean areas have complex geography. They are located in a relatively active seismic zone and their crust present several seismic faults. This paper presents a numerical study to assess slope stability in Lebanon under seismic loading. The study was performed using FLAC3D commercial software and the effect of several main parameters has been studied. These parameters include the soil behavior (elastic versus plastic behavior), soil friction angle, cohesion, earthquake frequency and others. Also, a case study was conducted to compare results generated from different examples of earthquakes. A Harmonic earthquake from Kocaeli and Chichi cases were considered for this purpose. The simulation results were presented in terms of the soil permanent displacement, the amplification of the soil particles velocity along the slope and the failure surface. The results show that the plastic behavior of soil represents better the true performance of soil slopes when subjected to earthquake loading. In addition, the results show that when the soil cohesion, the soil friction and the frequency of earthquake increase, the horizontal and the vertical displacement of the soil particles in the slope decrease and the slope becomes more resistant to failure and more stable.

INTRODUCTION

Slope failure, a natural disaster that occurs around the world, can be induced by earthquake loadings and can lead to severe damage/destruction in properties and loss of lives. For example, Chichi-Taiwan 1999's earthquake (Ms=7.6) destroyed 8500 buildings, heavily damaged about 6200 others, generated thousands of landslides and left 100,000 people homeless.

Lebanon and the Mediterranean area are located in an active seismic zone that increases the failure risk of naturally sloped soils. This has led to a continuously increasing interest in the analysis of slope stability under seismic loading.

The overstress of a slope or the reduction in the shear strength of its soil may cause a slope to displace. Engineers analyze slope to calculate quantitative indicators of performance such as factor of safety, lateral deformation, probability of failure and reliability index. Slope stability analysis includes

[1]Graduate Student, Rafik Hariri University, Meshref, Lebanon, ismailsa@students.rhu.edu.lb
[2]Professor, Lebanese University-University-Institute of Technology, Saida, Lebanon, fchehade@ul.edu.lb
[3]Assistant Professor, Rafik Hariri University, Meshref, Lebanon, wardanyrk@rhu.edu.lb

static and dynamic stability of earth slopes, natural slopes, cut slopes, embankments, landslides, etc. These slopes can be formed out of soil or rock.

Limit equilibrium method and slices-based method, which are more traditional methods, are used in the analysis in the stability og soil slopes under seismic loading. These methods have their own strengths and limitations. On the other hand, the latest technique of numerical modelling is another way of analysing soil slopes and can be used to solve complex slope geometries when the slope is subjected to several types of loading. The method allows for the determination of the stress and strain distribution at any point of a pre-defined grid.

SCOPE OF WORK

This paper presents a full static and dynamic analysis carried out on a seismic silty sandy soil slopes using finite difference method. Several parameters were studied which include: the soil behavior (elastic versus plastic behavior), the soil cohesion, the soil friction angle and the loading frequency. The results were presented in terms of the soil factor of safety (FOS), the horizontal displacement of soil particles (xdisp), the velocity amplification of soil particles along the slope (amplification) and the surface of failure.

SOFTWARE USED

A numerical modelling code, FLAC3D, "Advanced, Three-Dimensional Continuum Modelling for Geotechnical Analysis of Rock, Soil and Structural Support" , was used in this study. FLAC3D uses finite difference models that represent complex behavior not suited to finite element models such as non-linear material behavior, unstable systems and large displacement and strains, and so on. The software allows for simulating behavior of structures built of soil, rock or other materials that may undergo plastic flow when their yield limits are reached. The materials are represented by elements or zones, which form a grid that can be adjusted by the user.

ANALYSIS AND RESULTS

1- Factor of Safety

The Factor of Safety, FOS, is an indicator used to study the state of stability of soil slopes. Several definitions of FOS were given by authors like Bishop (1995), Matsui & San (1992) and Dawson & Roth (1999). The Factor of Safety is equal to the forces that resist slope movement over those that drive the movement. In designing and analyzing slopes, FOS is generally taken equal or greater than 1.5 to assure that the slope will be safely stable. However, Guyer (2012) considers slopes to have an adequate assurance of safety when the factor of safety is greater or equal than 1.15-1.2 for transient loads such as earthquakes.

2- Modelling with FLAC3D

A silty sandy slope with a height of 20m and an inclination angle of 30° was created. A free field boundary condition 2m*2m mesh was used through the study to simulate the earthquake loading. Figure 1 and table 1 illustrates the geometry and the soil mechanical properties of the slope analyzed. Figure 2 shows the harmonic wave used in the analysis of the effect of the soil behavior and of the frequency. The frequency of this wave is 0.8Hz while the natural frequency of the soil is 0.87Hz. Figure 3 shows Kocaeli's earthquake wave (Ms=7.4) that was used in the dynamic analysis of the soil cohesion and the soil friction angle and figure 4 shows Chichi's earthquake wave (Ms=7.6) that was used in the comparison of the effect of the different earthquake loading types.

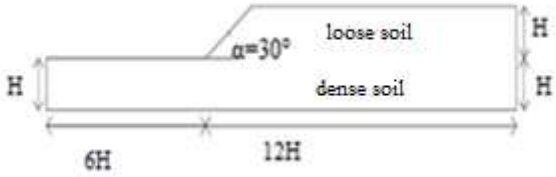

Figure 1: The slope geometry

Table 1: The slope mechanical properties

Reference (H=20m)	Dense Soil	Loose Soil
Elastic modulus (Pa)	$900*10^6$	$25*10^6$
Poisson's ratio ϒ	0.25	0.3
Shear modulus (Pa)	$400*10^6$	$9.6*10^6$
Bulk modulus (Pa)	$666.66*10^6$	$20.83*10^6$
Cohesion (Pa)	$2*10^5$	$5*10^3$
Friction angle (°)	35	30
Dilation angle ψ(°)	3	9

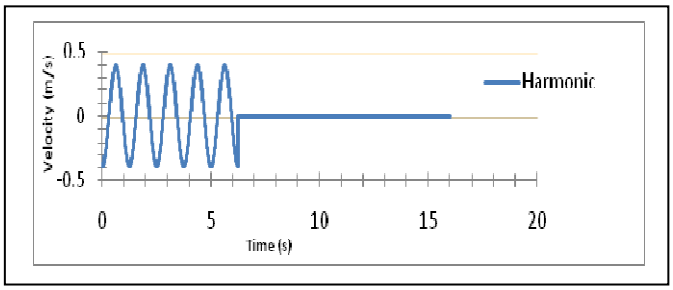

Figure 2: Harmonic wave speed with respect to time

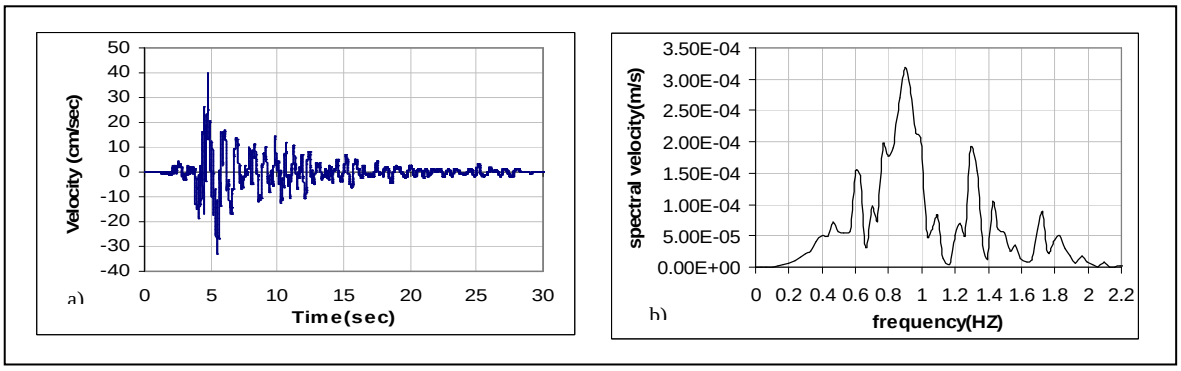

Figure 3: Kocaeli's earthquake, Turkey 1999: a) Velocity with respect to time and b) Spectral velocity with respect to frequency

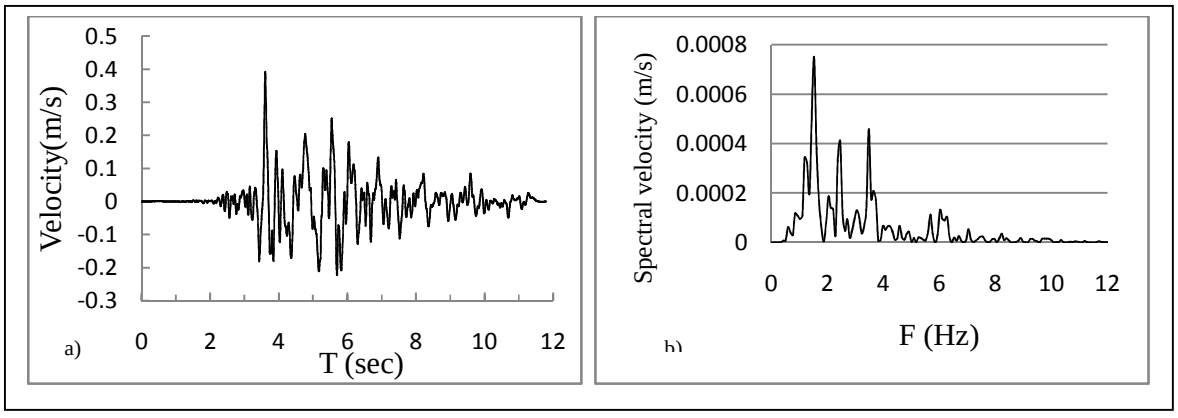

Figure 4: Chichi's earthquake, Taiwan 1999: a) Velocity with respect to time and b) Spectral velocity with respect to frequency

3-Results of the Static Analysis

The analysis discussed the effect of the soil cohesion (table 2) and the soil friction angle (table 3) on the slope factor of safety as shown in figure 5. The results show that:

- As the cohesion value of the loose soil is increased, the FOS is increased: c2 and c3 show a 16% and an 89% difference with respect to the reference case c1.
- As the friction angle value of the loose soil is increased, the FOS is increased: f2 and f3 show a 16% and an 18% difference with respect to the reference case f1.
- The FOS does not change when changing the cohesion or the friction angle value of the dense soil; it stays 1.42.

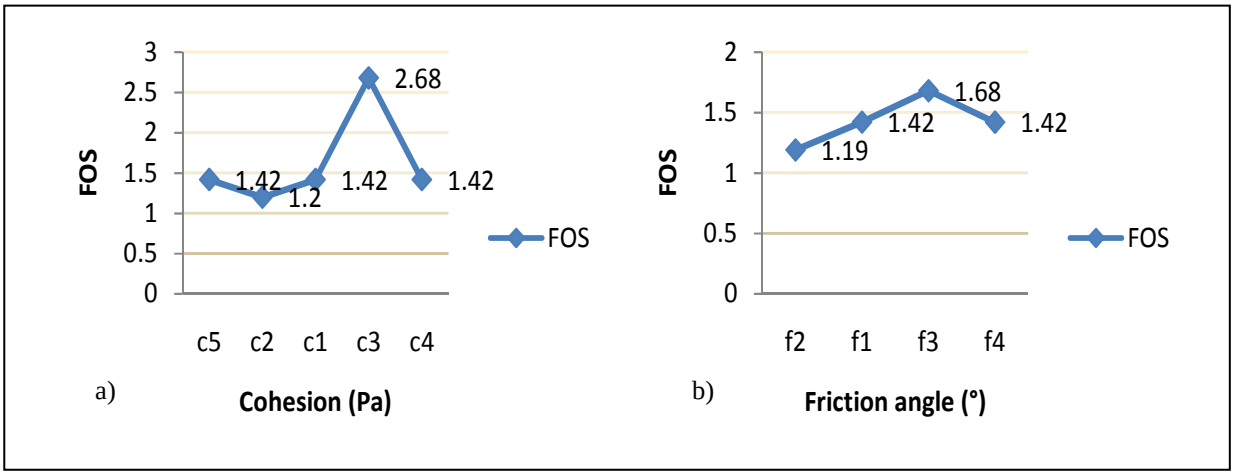

Figure 5: The variation of the FOS with respect to: a) soil cohesion and b) the soil friction angle

Table 2: The cohesion values of the 5 studied cases

Unit (Pa)	Case 1 (c1)	Case 2 (c2)	Case 3 (c3)	Case 4 (c4)	Case 5 (c5)
Loose soil	$5*10^3$	$0.5*10^3$	$50*10^3$	$5*10^3$	$5*10^3$
Dense soil	$2*10^5$	$2*10^5$	$2*10^5$	$4*10^5$	$1*10^5$

Table 3: The friction angle values of the 4 studied cases

Unit (°)	case 1 (f1)	Case 2 (f2)	Case 3 (f3)	Case 4 (f4)
Loose soil	30	20	35	30
Dense soil	35	35	35	40

4-Results of the Dynamic Analysis

4.1-Effect of Material Behavior

Figure 6 a) shows the soil particle displacement at bottom, middle and top of the slope in terms of time along the horizontal direction (x) for elastic and plastic behavior of soil under harmonic loading. Figure 6 b) shows the amplification at maximum for elastic and plastic behavior of soil under harmonic loading. Figure 7 a) shows the failure circle at Elastic Harmonic and b) Plastic Harmonic behavior of soil under harmonic loading. The results show that:

- At the elastic case, the maximum occurs at top then at middle then at bottom with 0.43m at 4.76s at bottom, -0.26m at 4.1s at middle and -0.08m at 0.3s at bottom. Also, the elastic case shows no permanent displacement at the end of the loading. At the plastic case, the maximum

permanent displacement occurs at middle then at top then at bottom with -2.78m at middle, -2.45m at top and without a permanent displacement but a maximum of -0.08 at 0.3s at bottom. The behavior of the plastic case is almost the same as the behavior of the elastic case at bottom as shown by figure 6 a).

- The maximum amplification of the soil particles velocity along the slope value is greater at the elastic case with a value of 3.34 than at the plastic case with a value of 2.22 as shown by figure by figure 6 b).
- The elastic case shows no failure circle while the plastic case shows a failure circle with the centre located at ($1.77*10^{2}$,$5*10^{-1}$,$2*10^{1}$) ((x,y,z)) and a radius of $9.9*10^{2}$m. The xdisp contour of the failure circle varies between the range of ($-7.7936*10^{-1}$, $-7.5*10^{-1}$) to the range (0, $4.8662*10^{-3}$) with an interval of $5*10^{-2}$ as shown by figure 7.

In reality, the impact of a loading leaves a remarkable permanent displacement at middle and top of a slope. Also, a failure circle along the slope is produced. This is shown in the plastic not the elastic case. Thus, the plastic case reflects better the true behavior of soil than the elastic case and is adopted in the analysis of the slope stability parameters.

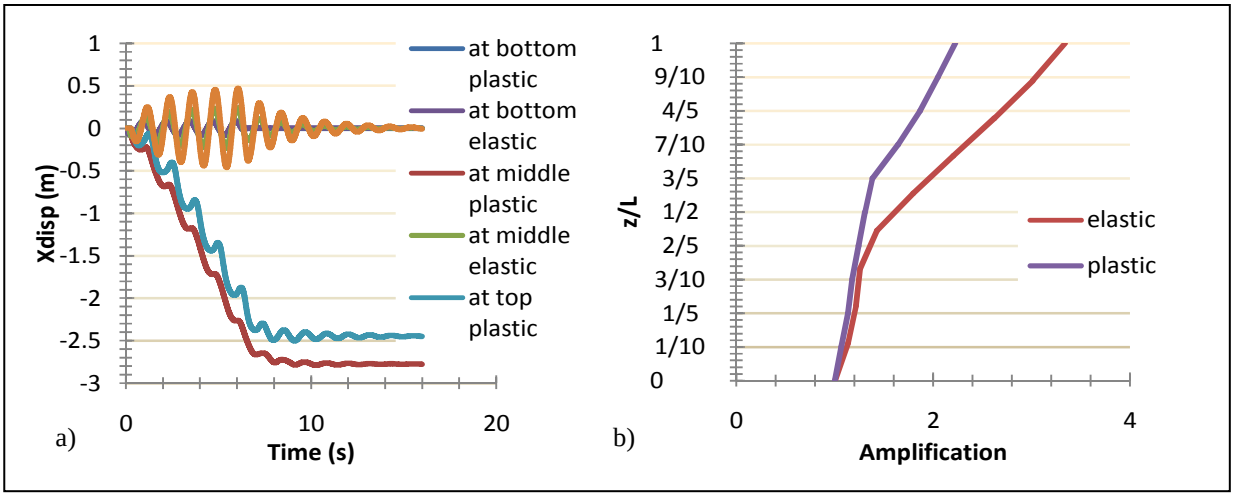

Figure 6: a) Xdisp at bottom of slope, at middle and at top for elastic and plastic behavior of material under harmonic loading and b) maximum amplification of the particle velocity along the slope for elastic and plastic behavior under harmonic loading

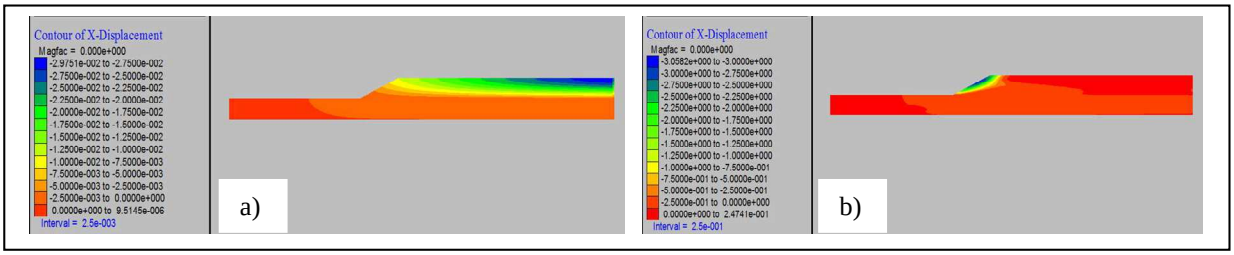

Figure 7: Failure circles: a) Elastic soil behavior under harmonic loading b) Plastic soil behavior under harmonic loading

4.2-Effect of Frequency

Figure 8 a) shows the displacement of soil particles at middle and top of the slope in terms of frequency along the horizontal direction (x) under harmonic loading and b) shows the maximum amplification of the soil particles velocity along the slope for the effect of frequency under harmonic loading. The results show that:

- The maximum permanent displacement at middle of the soil slope is at f=0.7Hz with -3.5m then at f=0.6Hz with -3.21m then at f=0.4Hz with -3.08m then at f=0.8Hz with -2.78m then at

f=0.9Hz with -1.94m then at f=1Hz with -1.35m then at f=1.5Hz with -0.38m as shown in figure 8 a).

- The maximum permanent displacement at top of the soil slope is at f=0.7Hz with -3.21m then at f=0.6Hz with -2.93m then at f=0.4Hz with -2.71m then at f=0.8Hz with -2.45m then at f=0.9Hz with -1.62m then at f=1Hz with -1.03m then at f=1.5Hz with -0.10m as shown in figure 8 a).
- The maximum amplification of the soil particles velocity along the slope is at f=0.8Hz with 2.22 then at f=0.9Hz with 2.06 then at f=0.7Hz with 1.99 then at f=1Hz with 1.79 then at f=0.6Hz with 1.61 then at f=1.5Hz with 1.35 then at f=0.4Hz with 1.23 as shown in figure 8 b).

The natural frequency of the soil is equal to 0.86Hz. Thus, the horizontal displacement and amplification of the soil particles velocity along the slope increase as the loading frequency becomes closer to the soil natural frequency.

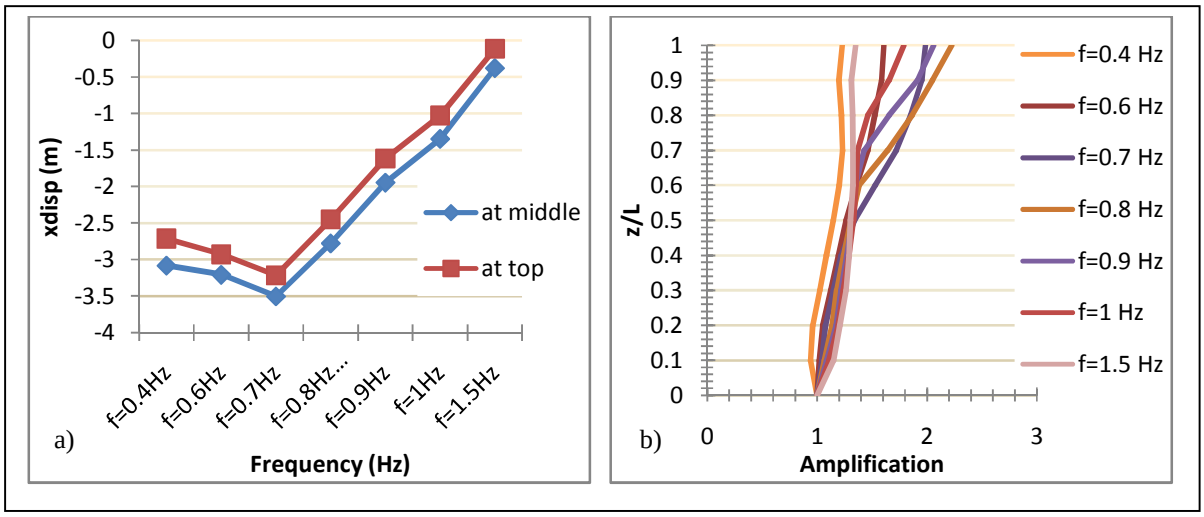

Figure 8: a) Xdisp at middle and at top under seismic loading with respect to Frequency and b) maximum amplification of the particle velocity along the slope for the effect of loading frequency under seismic loading

4.3-Effect of Soil Cohesion

Figure 9 a) shows the displacement of soil particles at middle and top of the slope in terms of soil cohesion along the horizontal direction (x) under seismic loading and b) shows the maximum amplification of the soil particles velocity along the slope for the effect of soil cohesion under seismic loading. The results show that:

- The maximum permanent displacement at middle of the soil slope is at c2 curve with -2.10m then at c4 curve with -0.777m then at c1 curve with -0.753m then at c5 curve with -0.722m then at c3 curve with -0.05035m as shown in figure 9 a).
- The maximum permanent displacement at top of the soil slope is at c2 curve with -1.82m then at c4 curve with -0.468m then at c1 curve with -0.457m then at c5 curve with -0.434m then at c3 curve with 0.00710m as shown in figure 9 a).
- The maximum amplification of the soil particles velocity along the slope is at c3 with 1.25 then at c5 with 1.23 then at c1 and c2 with 1.15 then at c4 with 1.059 as shown in figure 9 b).

Thus, for loose soil, as the cohesion value increases, the horizontal displacement of the soil particles decreases while for dense soil, as the cohesion value decreases, the horizontal displacement of the soil particles slightly decreases. As for the amplification of the soil particles velocity along the

slope, it decreases when the loose soil cohesion value decreases and increases when the dense soil cohesion value decreases.

4.4-Effect of Soil Friction Angle

Figure 10 a) shows the displacement of soil particles at middle and top of the slope in terms of soil friction angle along the horizontal direction (x) under seismic loading and b) shows the maximum amplification of the soil particles velocity along the slope for the effect of soil friction angle under seismic loading. The results show that:

- The maximum permanent displacement at middle of the soil slope is at f2 with -1.355 m then at f4 with -0.755m then at f1 with -0.7526m then at f3 with -0.512m as shown in figure 10 a).
- The maximum permanent displacement at top of the soil slope is at f2 with -1.049m then at f4 with -0.4591m then at f1 with -0.457m then at f3 with -0.214m as shown in figure 10 a).
- The maximum amplification of the soil particles velocity along the slope is at f3 with 1.17 then at f1 with 1.15 then at f2 with 1.14 then at f4 with 1.13 as shown in figure 10 b).

Thus, as the friction angle value increases, the horizontal displacement of the soil particles decreases and the amplification of the soil particles velocity along the slope increases.

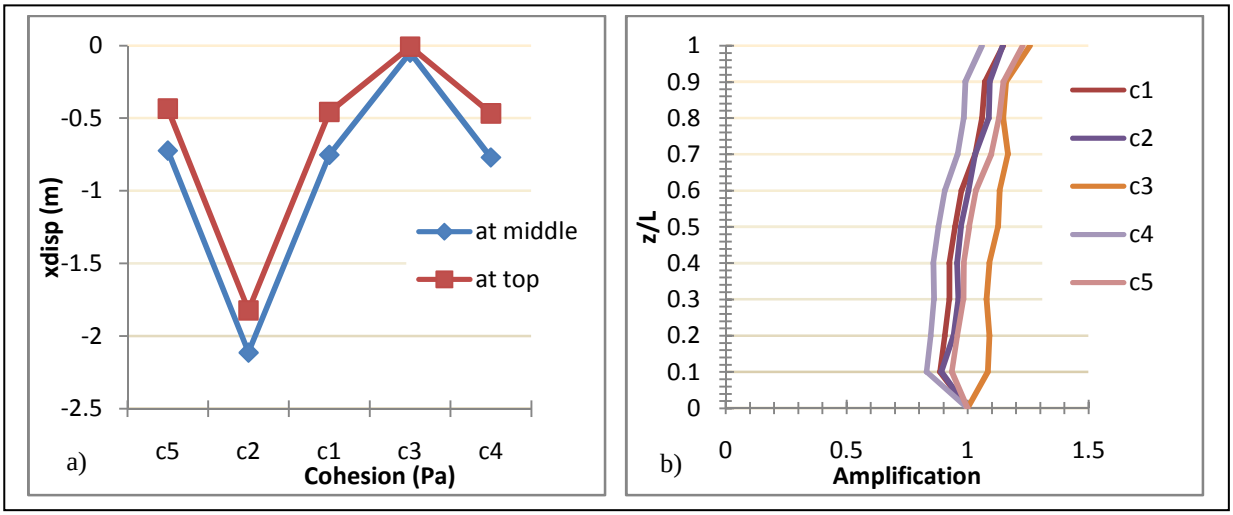

Figure 9: a) Xdisp at middle and at top under seismic loading with respect to cohesion and b) maximum amplification of the particle velocity along the slope for the effect of soil cohesion under seismic loading

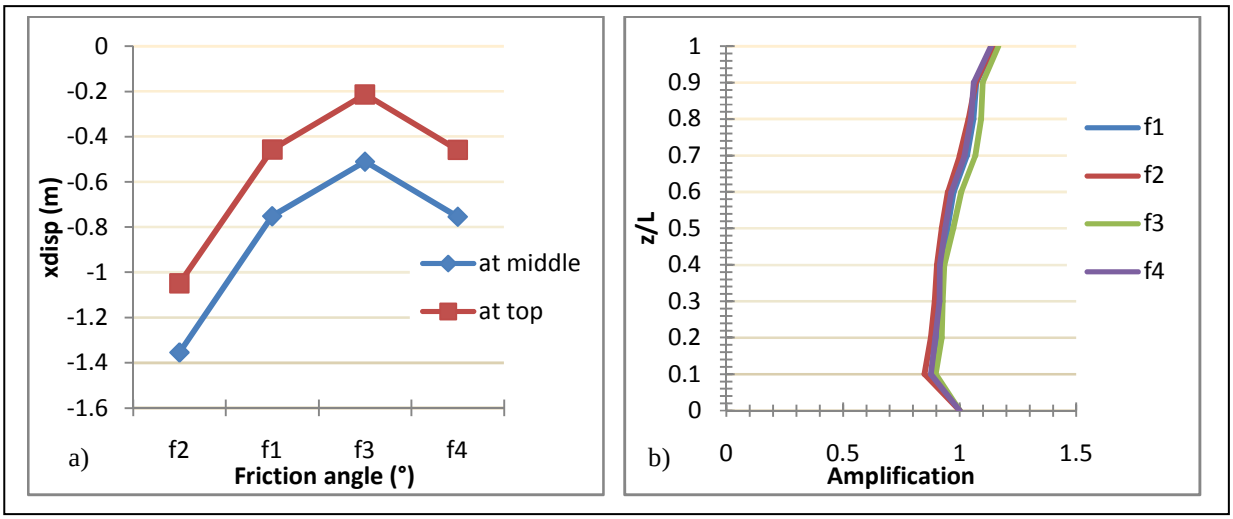

Figure 10: a) Xdisp at middle and at top under seismic loading with respect to friction angle and b) maximum amplification of the particle velocity along the slope for the effect of soil friction angle under seismic loading

4.5-Effect of Earthquake Loadings

Figure 11 a) shows the displacement of soil particles at middle and top of the slope in terms of earthquake loadings along the horizontal direction (x) under seismic loading and b) shows the maximum amplification of the soil particles velocity along the slope for the effect of earthquake loadings under seismic loading. Table 4 shows the peak frequency of the earthquake waves for the effect of earthquake loadings. The results show that:

- The maximum permanent displacement at middle of the soil slope is at Harmonic with -2.78m then at Kocaeli's earthquake with -0.755m then at Chichi's earthquake with -0.627m as shown in figure 11 a).
- The maximum permanent displacement at top of the soil slope is at Harmonic with -2.45m then at Kocaeli's earthquake with -0.453m then at Chichi's earthquake with -0.326m as shown in figure 11 a).
- The maximum amplification of the soil particles velocity along the slope is at Harmonic with 2.22 then at Kocaeli's earthquake with 1.15 then at Chichi's earthquake with 1.05 as shown in figure 11 b).

Thus, as the wave peak frequency increases, the horizontal displacement and amplification of the soil particles velocity along the slope decrease.

Table 4: Peak frequency of Harmonic, Kocaeli and Chichi' earthquake waves for the effect of earthquake loadings

	Peak Frequency (Hz)
Harmonic	0.8
Kocaeli	0.9
Chichi	1.5

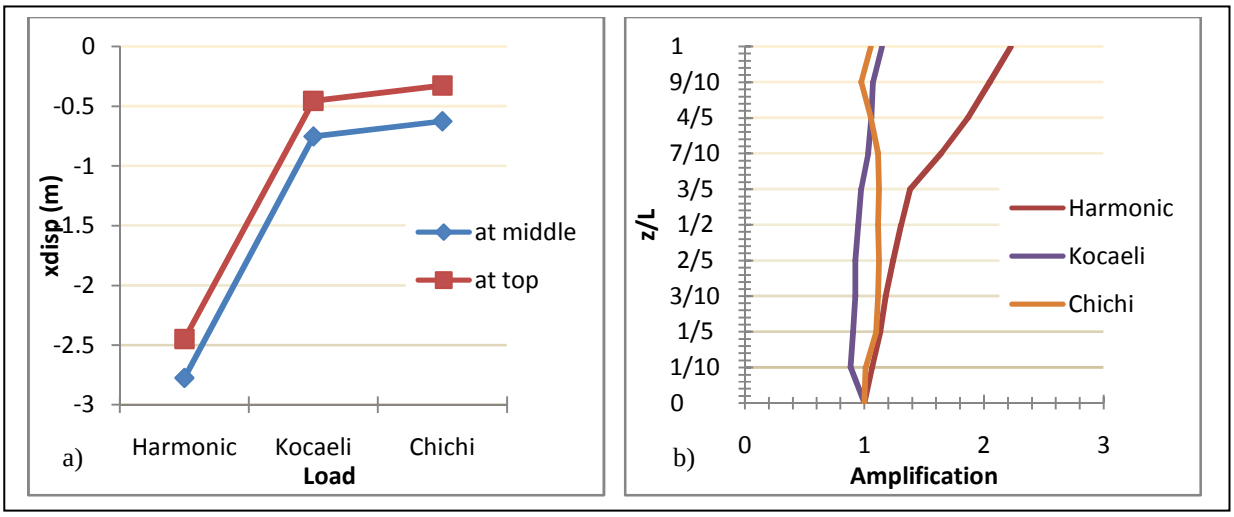

Figure 11: a) Xdisp at middle and at top under seismic loading with respect to Cohesion and b) maximum amplification of the particle velocity along the slope for the effect of earthquake loadings under seismic loading

CONCLUSIONS

This paper analyzed the stability of 20m height silty-sandy soil using finite difference. The following conclusions were drawn from the obtained results:

- The Factor of Safety of soil slopes against failure (FOS) increases with the increase in the cohesion value and friction angle of the soil forming the slope.
- The in situ compactness (dense versus loose) of the soil bearing the slope (below the slope), does not appear to affect the stability of the upper soil slope when subjected to seismic loading.
- The plastic model of soil slope represents better the true behavior than the elastic model.
- In loose silty-sandy soil slopes:
    - The horizontal displacement and velocity amplification of the soil particles under seismic loading decrease with the increase in the soil cohesion.
    - The horizontal displacement of the soil particles under seismic loading decreases with the increase in the soil friction angle while the velocity amplification of the soil particles under seismic loading decreases with the increase in the soil friction angle.
    - The horizontal displacement and velocity amplification of the soil particles under seismic loading decrease with the increase in the wave peak frequency.

REFERENCES

Bishop A.W. (1995) “The use of slip circle in the stability analysis of slopes” *Geotechnique, 4 (1995) 7-17.*

Chowdhury R, Flentje P, Bhattacharya G.(209) Geotechnical Slope Analysis, CRC Press Taylor And Francis London, UK.

Das B.M. (209) Principles of Geotechnical Engineering, seventh edition, Cengage Learning, USA

Dawson E.M, Roth W.H, Drescher A “Slope stability analysis by strength reduction” *Geotechnique, 49 (1999) 835-840.*

Guyer J.P, P.E, R.A (2010) “Continuing Education and Development”, Inc. 9 Greyridge Farm Court Stony Point, NY 9980

Itasca Consulting Group Inc. (2003) “FLAC3D3D (fast Lagrangian analysis of continua in 3 dimensions) user’s manual”, (version 2.1). Minneapolis,USA: Itasca Consulting Group Inc.

Kourdey A, AIheib M and Piguet J.P (2001) “Evaluation of Slope Stability by Numerical Methods”, *17th International Mining Congress and Exhibition of Turkey- IMCET2001, ISBN 975-395-417-4 , LAEGO - Nancy School of Mines-France.*

Matsui T., San K.C "Finite element slope stability analysis by shear strength reduction technique", *Soils Found, 32 (1992) 59-70.*

Nielson A. H (2006) "Absorbing Boundary Conditions For Seismic Analysis In ABAQUS", *2006 ABAQUS Users' Conference.*

Risk Management Solutions, I n c. (2000) https://support.rms.com/publications/turkey_event.pdf

Risk Management Solutions, I n c. (2000), https://support.rms.com/publications/Taiwan_Event.pdf

Stead D, Fraser S, Eberhardt R, Coggan J and Benko B (2001) "Advanced Numerical Techniques In Rock Slope Stability Analysis – Applications And Limitations , Landslides – Causes, Impacts and Countermeasures" , *Davos, Switzerland, pp. 615-624*

Zhang Y, Chen G, Wu J, Zheng L, Zhuang X (2010) "Numerical simulation of seismic slope stability analysis based on tension-shear failure mechanism", *Geotechnical engineering journal of the SEAGS & AGSSEA, Vol. 43 No2 June 2010 ISSN 0046-5828.*

Zhang Y.B, Chen G.Q, Zen K, Kasama K, Dong S.M "Limit analysis of seismic slope stability based on tension-shear failure mechanism", *Preceedings, Slope Stability 2010: International Symposium on Rock Slope Stability in Open Pit Mining and Civil Engineering. 18-21, September 2010 Vancouver, Canada.*